1   **Tangential streaming potential, transmembrane flux, and chemical cleaning of ultrafiltration**

2   **membranes**

3   Elizabeth Arkhangelsky[1,2,3]*, Aimira Bazarbayeva[1,2], Arailym Kamal[1,2], Jong Kim[1], Vassilis

4   Inglezakis[2,3,4], Vitaly Gitis[5]

5   [1] Department of Civil and Environmental Engineering, Nazarbayev University, 53 Kabanbay Batyr Avenue, Nur-Sultan,
6   010000 Kazakhstan

7   [2] Environmental Science & Technology Group (ESTg), Nazarbayev University, 53 Kabanbay Batyr Avenue, Nur-Sultan
8   010000, Republic of Kazakhstan

9   [3] The Environment and Resource Efficiency Cluster (EREC), Nazarbayev University, 53 Kabanbay Batyr Avenue, Nur-
10   Sultan 010000, Republic of Kazakhstan

11   [4] Department of Chemical and Materials Engineering, School of Engineering, Nazarbayev University, 53 Kabanbay Batyr
12   Avenue, Nur-Sultan 010000, Republic of Kazakhstan

13   [5] Unit of Energy Engineering, Ben-Gurion University of the Negev, PO Box 653, Beer-Sheva 8410501, Israel

14   * To whom correspondence should be addressed. E-mail: yelyzaveta.arkhangelsky@nu.edu.kz

15

16   **Abstract**

17   Transmembrane flux measurements are the only practical tools used to evaluate the degree of

18   organic fouling and the efficiency of chemical cleaning of ultrafiltration membranes *in situ*. Tangential

19   pH-streaming potential profiles may become a comprehensive *in situ* method to analyse cleaning

20   efficiency versus potential membrane damage. A parallel implementation of the two methods was used

21   to assist in tuning an efficient cleaning protocol for 300 kDa polyethersulfone membranes. The

22   membranes were fouled with a mixture of organics and cleaned with nitric acid, acetic acid, caustic

23   soda or liquid bleach, each at concentrations of 1, 5, or 10 mg/L. A modified Kolmogorov-Smirnov

24   test for divergence in datasets clearly indicated cleaning with 5 mg/L NaOH or NaOCl. These findings

25   were confirmed by atomic force microscopy surface contouring and infrared spectra recording.

26   Tangential pH-streaming potential profiling is easy in terms of operation and maintenance,

27   inexpensive, and may be conducted *in situ.* Implementation of two independent tests is instrumental in

28   the validation of the cleaning agent efficiency, optimisation of the cleaning dose and pH, and

29   assessment of membrane fouling potential by complex organic mixtures. A combination of

30   transmembrane flux and tangential streaming potential tests may reduce the cost of chemical cleaning

31   and suspend membrane ageing.

32 **Keywords:** Ultrafiltration; Polyethersulfone; Atomic force microscopy; Attenuated total reflection

33 Fourier-transform infrared spectroscopy; Transmembrane pressure

34

1.   Introduction

Ultrafiltration (UF) membranes are routinely implemented to purify proteins for pharmaceutical and biotechnological needs [1,2]. The operation is typically conducted with polymer membranes that gradually become fouled by proteins. Maintaining a good protein yield and membrane selectivity requires the periodic cleaning of the fouled membranes. Physical cleaning is applied regularly to hydraulically remove reversible foulants via surface and back washing. Foulants lodged on the membrane surface after hydraulic cleaning are removed by chemical cleaning. Efficient chemical cleaning requires a suitable cleaning agent specific to the type of foulant. Acids are used to dissolve inorganic precipitates, bases are used for the hydrolysis of proteins, and oxidants are used for the oxidation of organics. Complex fouling is treated through a sequence of cleaning agents, as prescribed in cleaning protocols. The protocols are typically generic, derived empirically, kept within a chemical company, and rarely optimised [3]. The ultimate goal is to efficiently clean the membrane within a short period of time. To achieve this, high concentrations of cleaning agents and short contact times are usually implemented [4]. To increase cleaning efficiency, a protocol typically recommends 1) increasing the concentration of the cleaning agent, or 2) increasing the time/frequency of chemical cleaning, or 3) using more aggressive cleaning agents, or 4) magnifying the transmembrane pressure. The solutions are expensive (extended energy and water consumption, reduced production time), impact upon membrane integrity or accelerate its ageing, and ultimately impair the filtrate quality [5]. A treatment facility is then forced to replace the damaged membranes with new membranes sooner than would have been the case if an optimised cleaning protocol had been implemented. The replacement increases the operational expenses of membrane operation and the cost of the purified product.

The exact cleaning protocol has one major weakness; the evaluation of cleaning efficiency. A properly cleaned membrane should be intact and not exhibit any chemical or microbiological residues on its surface or within the matrix. In general, visual observations of the membrane surface, studies of its chemical composition by infrared (FTIR) spectroscopy, X-ray photoelectron (XPS) spectroscopy, energy dispersive X-ray (EDX) spectroscopy, or bacteriological tests for microbial fouling, are conducted *in situ* using sophisticated equipment and are avoided. There are two *in situ* analyses that are routinely conducted to assess the efficiency of chemical cleaning; hydraulic and bubble point tests. The bubble point test [6] verifies the appearance of pores larger than 1 μm, while the hydraulic test usually determines cleaning efficiency as a ratio of transmembrane fluxes through a fouled and a pristine membrane. A hydraulically clean membrane is the one that shows an arbitrary ratio of 0.65

67   [7], 0.87 [8], 0.95 [9–12], or any other number that may eventually be even higher than 1.0. And still,,

68   a membrane can demonstrate complete flux recovery while foulants are deployed on its surface and

69   within the matrix [13]. Aggressive chemical cleaning, particularly if the membrane is fouled by

70   organic matter, affects the bonds between the foulants and the membrane. As the membrane and the

71   residue are of organic origin, the cleaning agent often oxidises the membrane itself. Membrane

72   oxidation increases its hydrophilicity, surface charge, and pore size [14]. An increased hydrophilicity

73   or surface charge will compensate for partial flux loss due to irreversible fouling, especially during the

74   initial stages of its development. Inaccurate assessment based on insufficient knowledge leads to

75   continued membrane operation despite the membrane being partially fouled. Potential organic foulants

76   use existing fouled sites as stepping stones for further invasion of the membrane surface until there is

77   excessive coverage. At this stage, the flux cannot be recovered, and the membrane needs to be

78   replaced. This situation may be prevented if an additional *in situ* non-invasive test would properly

79   interpret the assessment of membrane status and the chemical cleaning effectiveness. Although the

80   hydraulic test is essential, it alone is insufficient.

81   This study suggests an additional *in situ* monitoring technique to understand the chemical cleaning

82   acquired by flux measurements. The streaming potential originates when an electrolyte solution moves

83   over a charged surface, and the motion is induced by a hydrostatic pressure gradient. The

84   measurements are non-destructive and may be conducted either by forcing the electrolyte through the

85   membrane pores (transmembrane streaming potential) or alongside the membrane surface (tangential

86   streaming potential). This approach is not novel and has been widely discussed more than a decade ago

87   [15–23]. However, the approach has not been advanced as studies suggested measuring a

88   transmembrane streaming potential when the flow was directed perpendicular to the active membrane

89   layer. In case of cake formation as the main fouling mechanism, measurements do not reflect the real

90   properties of the cake layer, as the membrane itself plays a non-negligible role [24]. Studies that

91   reported tangential streaming potential measurements used impractically high concentrations of

92   cleaning agents [25,26] and mainly reported on changes in the streaming potential values as a result of

93   cleaning. The use of tangential streaming potential sequencing to optimise the dose of a cleaning agent

94   has not previously been reported in the literature.

95   To the best of our knowledge, the capacities of the tangential streaming potential have not been

96   fully explored, particularly to distinguish between a clean and an affected membrane. A sufficiently

97   cleaned membrane exhibits a tangential pH-streaming potential profile close to that of a virgin

98   membrane. If the flux through a cleaned membrane is equal to its initial value, but the pH-streaming

99   potential profile is different from that of a virgin membrane, the membrane is damaged or has not been

100 sufficiently cleaned. Confirmation of this hypothesis will equate the definition of a hydraulically clean

101 membrane with the definition of a chemically cleaned membrane. It is important to remember that

102 industrial users are interested in methods that are *in situ*, inexpensive, and easy to operate and

103 implement. Streaming potential has the capacity to become a fundamental tool to monitor chemical

104 cleaning and provide necessary feedback control of its efficiency. The proposed test is suitable for a

105 variety of UF separation processes, including water and wastewater treatment. Efficient

106 implementation of the proposed monitoring technique will require tuning based on the nature of the

107 filter cake that will be formed during the process.

2. Materials and methods

2.1. Membrane preparation and characterisation

110 New 300 kDa polyethersulfone (PES) membranes (Sterlitech Corporation, USA) were used. Prior to

111 the first use, membranes were shaken in a shaker at 37 °C for 1 h. The shaking resulted in similar feed

112 and permeate total organic carbon (TOC) levels during the filtration of deionised water (DIW, MilliQ

113 quality). Zeta potential was measured using a SurPASS electrokinetic analyser (Anton Paar GmbH,

114 Austria). The pH was varied from 2 to 10 automatically, and each specific zeta potential value was

115 measured twice. DIW was used to prepare the electrolytes, and all solutions used to regulate ionic

116 strength (KCl) and pH (KOH, HCl) were of analytical grade. The membrane contact angle was

117 measured with an optical contact angle (OCA) 25 (DataPhysics Instruments GmbH, Germany) contact

118 angle metre using sessile DIW drops. Eight to ten measurements with separate membrane pieces per

119 sample were conducted. The reported values were the arithmetic means of all measurements.

120 Attenuated total reflectance Fourier-transform infrared (ATR-FTIR) spectra were obtained using a

121 Cary 660 FTIR spectrometer (Agilent, USA); all spectra were recorded at ambient temperature. The

122 instrument was purged with dry nitrogen to prevent the interference of atmospheric moisture.

123 Membrane samples were kept in closed Petri dishes filled with water and blotted dry prior to analysis.

124 Excess water was removed by drying in a desiccator over P_2O_5 for 2 h. Wavenumbers between 400 and

125 $4000 \, cm^{-1}$ were recorded with a 4 cm^{-1} resolution. Atomic force microscopy (AFM) SartSPM 1000

126 (AIST-NT Inc., USA) was used for visual analysis of membrane surfaces.

2.2. Filtration experiments

128 Filtration experiments were conducted in a CF016 cross-flow stainless steel cell (Sterlitech

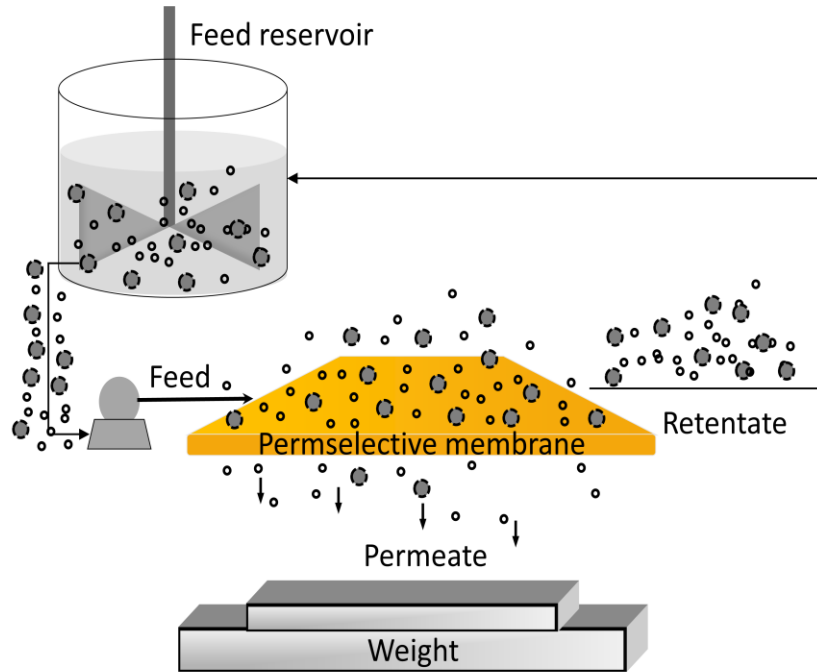129 Corporation, USA) with a 16 cm^2 internal filtration area; Figure 1 illustrates the experimental setup.

130

131   Figure 1. Filtration cell setup.

132   Feed was supplied with a peristaltic pump (Cole –Parmer USA). The membranes were first compacted

133   for 30 min at 70 L/m^{2}h (LMH) transmembrane flux of DIW. The 60 min filtration cycles at a constant

134   transmembrane pressure (TMP) of 1.9 bar were conducted with 0.6 g/L Similac 1 baby formula

135   (Abbott Laboratories, USA) mixed in DIW. According to the manufacturer, the feed contains 65 mg/L

136   total proteins, 158 mg/L fat, and 348 mg/L carbohydrates. The transmembrane flux was calculated

137   gravimetrically as per Equation (1):

138     $$J = \frac{\Delta m}{\rho S \Delta t}$$ (1)

139   where Δm is the permeate weight difference (kg) measured with a digital balance (Kern, Germany); Δt

140   is the frequency interval (h); S is the active membrane surface area (0.0016 m^2); and ρ is the permeate

141   density (~1000 kg/m^3). Changes in flux due to cake formation were calculated as per Equation (2)

142   [27]:

143     $$J/J_0 = \left(1 + \frac{2\alpha St}{\mu R_M^2} TMP\right)^{-1/2}$$ (2)

144   where J_0 is the flux through a pristine membrane; α is a parameter characterising the fouling potential

145   of the solution (4.5–6.5•10^5 m^{-4}); μ is the dynamic viscosity of water (10^{-3} kg/m·s); and TMP is

146    $1.9 \cdot 10^5$ Pa. The intrinsic membrane resistance R_M ($1.1 \cdot 10^{13}$ m^{-1}) was calculated using Equation (3)

147   [28]:

148    $$R_M = \frac{TMP}{\mu J_0} \tag{3}$$

149   The changes in flux due to internal pore plugging [27] assume that the membrane pores are plugged

150   due to the deposition or adsorption of organics within the pores:

151    $$J/_{J_0} = \left(1 + \frac{J_0 \beta t}{\varepsilon \lambda}\right)^{-2} \tag{4}$$

152   where ε (0.16) is membrane porosity; λ (10^{-7} m) is membrane thickness; and β (1.4-$2.5 \cdot 10^{-10}$) is a

153   dimensionless parameter that determines the potential for the solution to provoke internal fouling.

2.3. Membrane cleaning

155   Membrane cleaning was conducted with 1, 5, and 10 mg/L of nitric acid (HNO$_3$), acetic acid

156   (CH$_3$COOH), caustic soda (NaOH), or liquid bleach (NaOCl). All chemicals were obtained from

157   Sigma Aldrich and were used as received. The cleaning in place (CIP) operation was a 5 min

158   procedure, and the calculated Ct values were 5, 25, and 50 mg·min/L. After 5 min, membranes were

159   rinsed with DIW. The efficiency of chemical cleaning was assessed by relative flux calculated as

160    $J_{0,clean}/_{J_{0,virgin}}$ where $J_{0,clean}$ and $J_{0,virgin}$ are the fluxes through a chemically cleaned and a virgin

161   membrane, respectively. The flux values are aggregate DIW fluxes recorded during the first 5 min of

162   the filter run. The flux during this time was stable and indicated an absence of significant fouling or

163   compaction.

164   In addition, cleaning efficiency was evaluated by interpreting the Kolmogorov-Smirnov test [29] for

165   the highest dissimilarities in the data recorded through flux or zeta potential measurements. The

166   dissimilarities were calculated by 1) separate calculations of the aggregate values of each dataset; 2)

167   calculations of differences between two independent datasets at each measurement point; and 3)

168   identifying the largest difference point between the two datasets. These steps were aimed at

169   determining the extent to which the two datasets were different from one another. In flux calculations,

170   a separate dataset was used for filtration with DIW, and six datasets were used corresponding to 6 h of

171   operation. Chemical cleaning after each hour was conducted, and we were able to determine the flux

172   after each cleaning and how close this was to the flux obtained after the initial fouling. A close

173   replication of fouling cycles indicated that the membrane surface had been sufficiently cleaned to

174   perform in exactly the same manner. A significant deviation in flux values indicates that the membrane

175   has not been sufficiently cleaned, or that it has been damaged by overcleaning and will be prone to
176   more significant fouling in the next run.

177   The zeta potential dissimilarity curves were calculated by comparing the difference in the zeta
178   potential values of pristine, fouled, and cleaned membranes. Higher dissimilarity indicates that the zeta
179   potential curves of virgin and cleaned membranes are significantly different from each other. A close
180   replication of zeta potential values indicates that the membrane was properly cleaned. A significant
181   deviation suggests insufficient cleaning or overcleaning that may damage the membrane. In addition,
182   this information was used to distinguish two datasets with very similar flux data patterns.

183   **2.4. Square-wave method to determine critical flux**

184   The reversibility of fouling is dependent on the foulant flux towards the membrane surface. Below a
185   certain value, known as the critical flux, fouling is reversible. Above the critical flux, fouling is
186   irreversible. The critical flux is the minimum flux that causes irreversible fouling on the membrane
187   surface [30,31]. Constant TMP during filtration at constant flux, or repeatable TMP profiles following
188   physical cleaning, indicates that the flux is below critical. The inability to stabilise TMP during
189   filtration, or higher initial TMP immediately after physical cleaning, signifies that fouling is
190   irreversible. Thus, filtration in the reversible fouling domain implies a linear correlation between the
191   flux and the TMP. A stepwise increase in the TMP results in a higher flux, while a stepwise decrease
192   in the TMP should set the flux to previously measured values. This hypothesis is central to the square-
193   wave filtration method [32,33]. Stepwise increases and reductions in the TMP produce the same flux
194   profiles in the reversible fouling domain for the same TMP values. The inability to reproduce a
195   previous profile indicates that the flux is above critical. This method is useful in fouling experiments to
196   accurately assess the critical flux value using stepwise TMP alterations with positive and negative
197   variations. The essentials of the test are depicted in Figure 2.

198
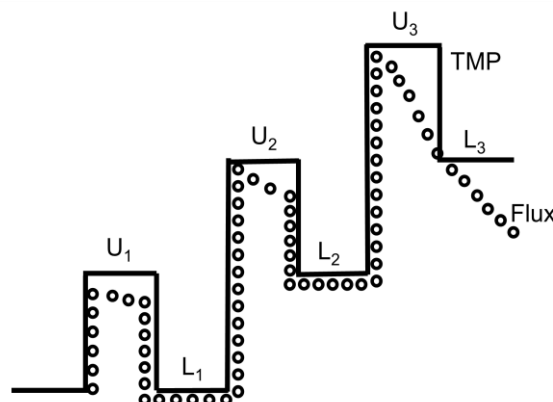
199   Figure 2. Principle of the square-wave method with stepwise pressure changes to upper (U_1, U_2, U_3)

200   and lower (L_1, L_2, L_3) values. Pressure values are denoted by the solid lines, and the flux values are

201   denoted by the dots. This scheme is modified from [32].

202   In Figure 2, the flux at the upper TMP levels, U_1 and U_2, is reversible, while the flux at U_3 is

203   irreversible. A test begins at a low constant TMP L_1 and shifts to a higher pressure (U_1), after a few

204   minutes. If the initial flux at U_1 is lower than at L_1, fouling is irreversible. If the flux at U_1 is higher

205   than at L_1, the test continues for several minutes, and the TMP is shifted back to L_1. If the flux L_1 after

206   L_1-U_1-L_1 sequence is stable and comparable to the flux at the first L_1, the fouling is reversible. Then,

207   the test proceeds to a higher TMP U_2 value, and continues until the flux enters the irreversible fouling

208   domain.

209   **3. Results**

210   The critical flux was determined using the square-wave method described in Section 2.4. Figure 3

211   depicts the evolution of fluxes and TMPs during the test.
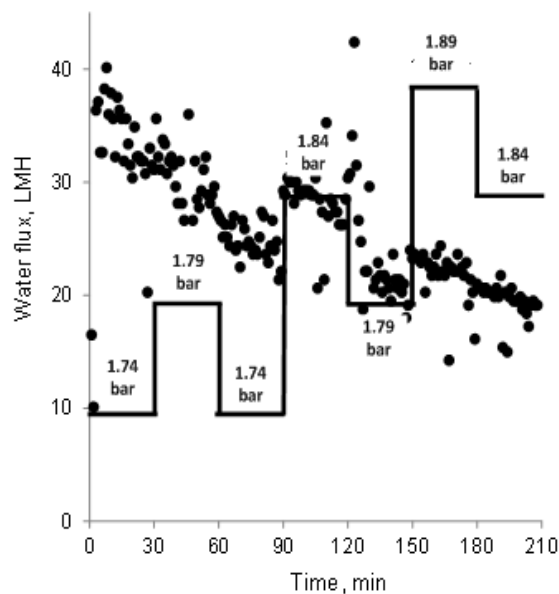

212

213   Figure 3. Evolution of flux and TMP during the irreversibility test. A continuous line represents the

214   applied TMP, and the dotted line represents the permeate flux.

215   During the first 30 min, the experiment was conducted at 1.74 bar TMP. The initial flux level of 10

216   LMH was replaced by a maximum of 40 LMH immediately after 5 min of filtration. Further, the flux

217   fluctuated between 40 and 30 LMH for the entire period. Values close to 40 LMH were observed at the

218   beginning of the run; they shifted towards 30 LMH at the end of the first period. After 30 min, the

219   TMP was shifted to 1.79 bar, although the expected increase in the flux was not observed. The flux

220   slowly decreased from 30 LMH near the beginning of the shift to 25 LMH towards the end of the

221   filtration period. The same values were measured when the TMP was shifted back to 1.74 bar. A shift

222   to 1.84 bar increased the flux towards 30 LMH with sporadic values close to 40 LMH. The shift back

223   to 1.79 bar displayed steady values around 20 LMH. A further increase towards 1.89 bar did not result

224   in a further increase in the flux; it remained stable around 20 LMH for the 1.89 and 1.84 bar periods.

225   Therefore, we concluded that 1.89 bar TMP is above the critical flux, and conducted further filter runs

226   at 1.9 bar TMP.

227   A typical filtration experiment is a sequence of six cycles; each cycle includes 1 h of PES 300

228   fouling and 5 min of chemical cleaning. The fouling was achieved using 0.6 g/L Similac 1 baby

229   formula that contained 65 mg/L total proteins, 158 mg/L fat, and 348 mg/L carbohydrates. The

230   cleaning was conducted with 1, 5, and 10 mg/L HNO_3, CH_3COOH, NaOH, or NaOCl. Virgin, fouled,

231   and cleaned membranes were characterised by flux, zeta potential, contact angle, ATR-FTIR, and

232   AFM. Figures 4 and 5 depict the flux changes of a fouled membrane cleaned by HNO_3, CH_3COOH,

233   NaOH, and NaOCl.
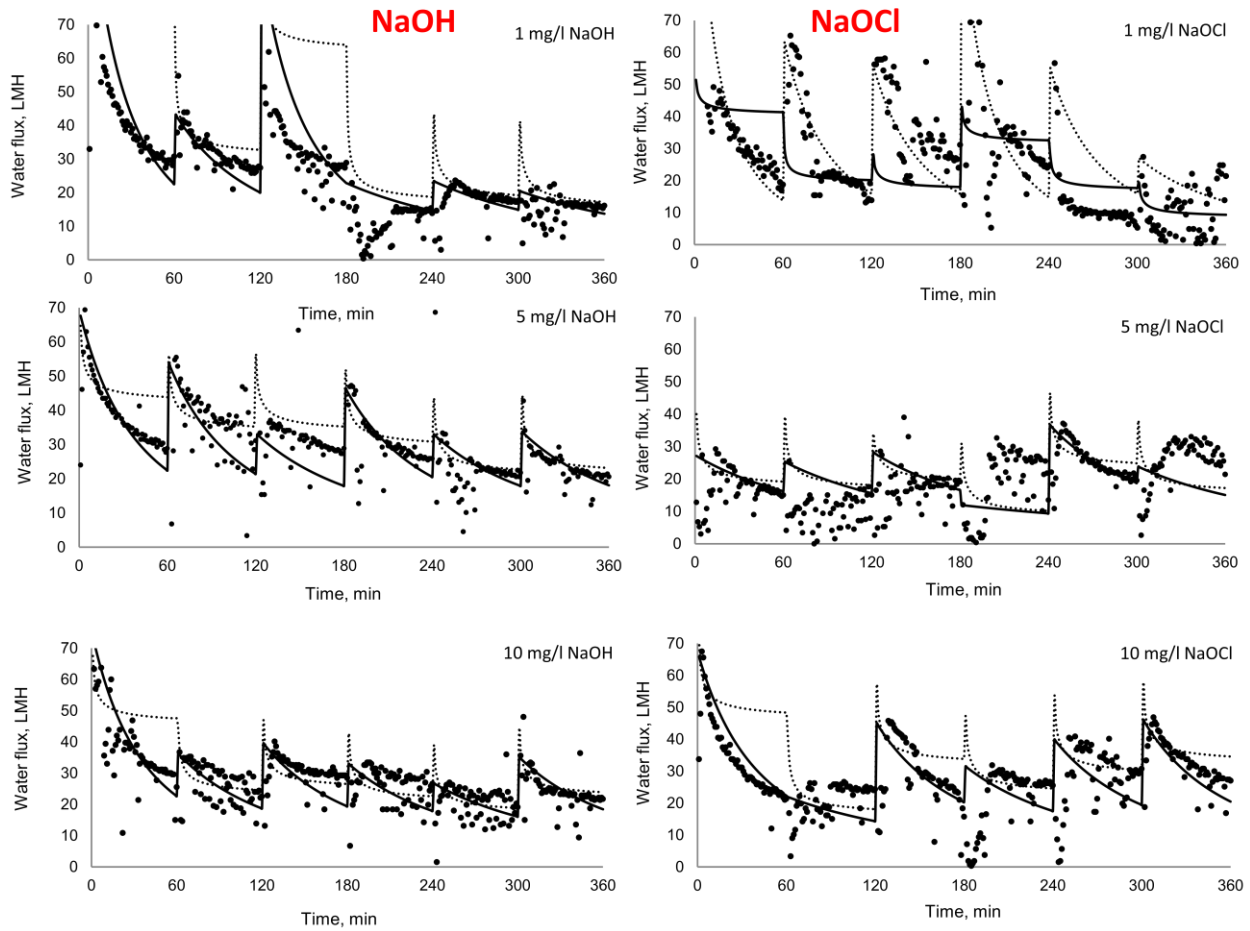
234
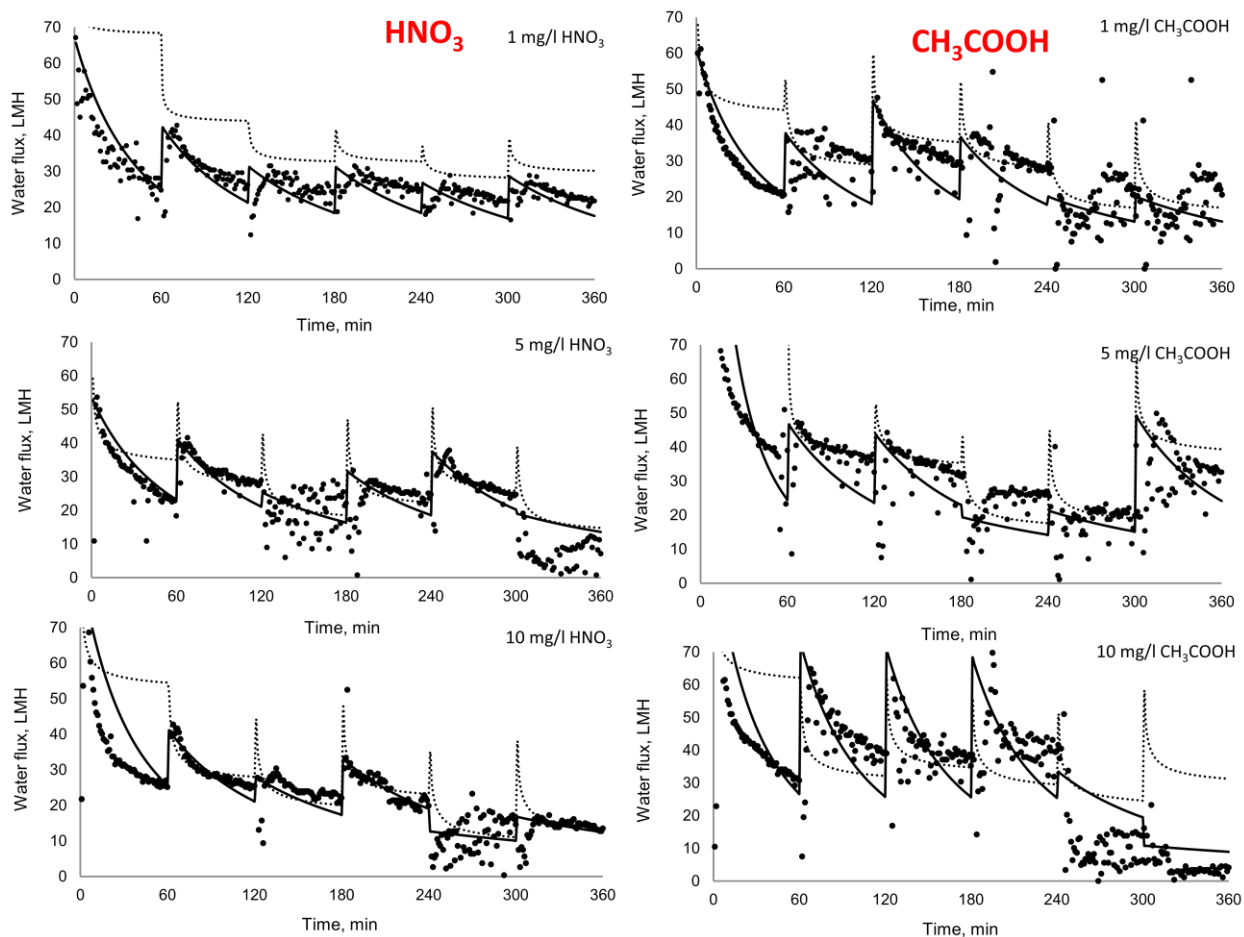
Figure 4. Evolution of flux as a function of filtration time through PES-300. Fouling with 0.6 g/L Similac 1 baby formula, cleaning with 5 (top), 25 (middle), and 50 (bottom) mg·min/L HNO_3 (left), and with 5 (top), 25 (middle), and 50 (bottom) mg·min/L CH_3COOH (right). Experimental data points are displayed as unconnected dots, a dashed curve is the best-fit approximation of flux behaviour due to cake formation, and a solid curve is a best-fit approximation of flux behaviour due to pore blocking (Equations (2) and (4), respectively). Here, R_M is $1.1 \cdot 10^{13}$ m^{-1}, TMP is $1.9 \bullet 10^5$ Pa, α is 4.5–$6.5 \bullet 10^5$ m^{-4}, β is 1.4–$2.5 \cdot 10^{-10}$, λ is 10^{-7} m, and μ is 10^{-3} kg/m·s.

242

Figure 5. Evolution of flux as a function of filtration time through PES-300. Fouling with 0.6 g/L

Similac 1 baby formula, cleaning with 5 (top), 25 (middle), and 50 (bottom) mg·min/L NaOH (left),

and with 5 (top), 25 (middle), and 50 (bottom) mg·min/L NaOCl (right). Experimental data points are

displayed as unconnected dots, a dashed curve is the best-fit approximation of flux behaviour due to

cake formation, and a solid curve is a best-fit approximation of flux behaviour due to pore blocking

(Equations (2) and (4), respectively). Here, R_M is $1.1 \cdot 10^{13}$ m^{-1}, TMP is $1.9 \cdot 10^5$ Pa, α is 4.5–$6.5 \cdot 10^5$ m^{-4},

β is 1.4–$2.5 \cdot 10^{-10}$, λ is 10^{-7} m, and μ is 10^{-3} kg/m·s.

250   All plots showed a significant drop in the transmembrane flux, from 70 to less than 30 LMH, during

251   the fouling of pristine membranes. The first cleaning successfully increased the flux to the 40–50 LMH

252   domain for all three *Ct* values. From here, the flux after HNO$_3$ cleaning gradually decreased towards

253   25 LMH at the end of the second filtration period. The second cleaning was much less successful and

254   did not increase flux above 30 LMH. High concentrations of the cleaning agents were more

255   destructive, and after four consecutive cleans, the flux through membranes cleaned with 5 and 10 mg/L

256   HNO$_3$ was barely 10 LMH. Cleaning with 1 mg/L HNO$_3$ maintained the flux slightly below 30 LMH,

257   while providing consistent and repeatable runs. Similar trends were observed when cleaning with low

258   concentrations of CH₃COOH. A gradual decrease in flux resulted in low flux after five to six cycles

259   that required a change in the cleaning regime or membrane replacement. Cleaning with a high

260   concentration of CH₃COOH was successful for the first four cycles. After that, the flux simply

261   dropped towards zero and was not recovered by cleaning.

262   The same pattern was observed when membrane was cleaned at low NaOH concentrations. After

263   three cleaning cycles with 5 mg/L·min the flux diminished towards 0 LMH and was restored after

264   cleaning to a stable 15 LMH level. Repeatable, although deteriorating, fouling patterns were observed

265   when the membrane was cleaned with 25 mg/L·min NaOH. After six cycles, flux dropped from 70 to

266   20 LMH and produced a stable fouling pattern. The flux after cleaning with 5 mg/L NaOH exhibited a

267   trend that was not as repeatable as that at previous concentrations, i.e. the initial flux of 70 LMH

268   rapidly reduced towards 20 LMH and remained stable after cycling.

269   The first clean with NaOCl restored the flux towards 65, 25, and 25 LMH for *Ct* values of 5, 25,

270   and 50 mg·min/L, respectively. Cleaning with 1 mg/L NaOCl resulted in a sporadic flux pattern when

271   immediately after cleaning, flux increased to 60 LMH although it ultimately reduced to 10–20 LMH

272   towards the next clean. Following the fourth clean, the initial flux was unable to increase above 30

273   LMH and fluctuated significantly between 10 and 30 LMH. The fifth clean indicated that the

274   membrane had completely fouled, and would not be able to operate any further using the same

275   cleaning protocol. Cleaning with 5 mg/L NaOCl resulted in a scattered flux pattern that fluctuated

276   between 30–35 LMH immediately after cleaning and was practically zero LMH at the end of the

277   filtration period. Cleaning with 10 mg/L NaOCl produced a well-defined pattern of flux reductions

278   towards 20 LMH immediately prior to cleaning, and flux increased toward 45 LMH immediately after

279   the clean. The interim conclusion is that a 5 min cleaning with 5 or 10 mg/L NaOH or NaOCl is

280   sufficient to secure continuous filtration. Cleaning with 10 mg/L appears preferable as it provides a

281   more consistent flux pattern with higher flux values. The flux after cleaning with 5 mg/L NaOCl was

282   observed to be chaotic and may increase the risk of further invasion of the membrane surface by

283   foulants.

284   Flux patterns demonstrated a gradual transition from pore blocking to cake formation as filtration

285   progressed. The first cycle displayed a significant flux decrease that fitted well with the anticipated

286   reduction due to pore blocking. Two different paths were observed from the second sequence onwards.

287   If chemical cleaning was successful, and the filtration path was restored, a flux pattern gradually

288   evolved from pore blocking to cake formation. The initial flux values of the second run were

289   comparable to each consecutive run, although the pattern was flatter and a better fit to the cake

290   approximation was seen clearly. The absence of a gradual transition to cake fouling indicates that the

291   membrane is continuously fouled and flux reduces till it becomes zero. Residual foulants assist in the

292   densification of a fouling layer from new foulants. Sufficient chemical cleaning removes the residual

293   foulants, exposing the membrane surface to new foulants. This trend was observed with ATR-FTIR,

294   AFM, and contact angle measurements.

295   Figure 6 presents the AFM micrographs of pristine, fouled, and cleaned PES-300.
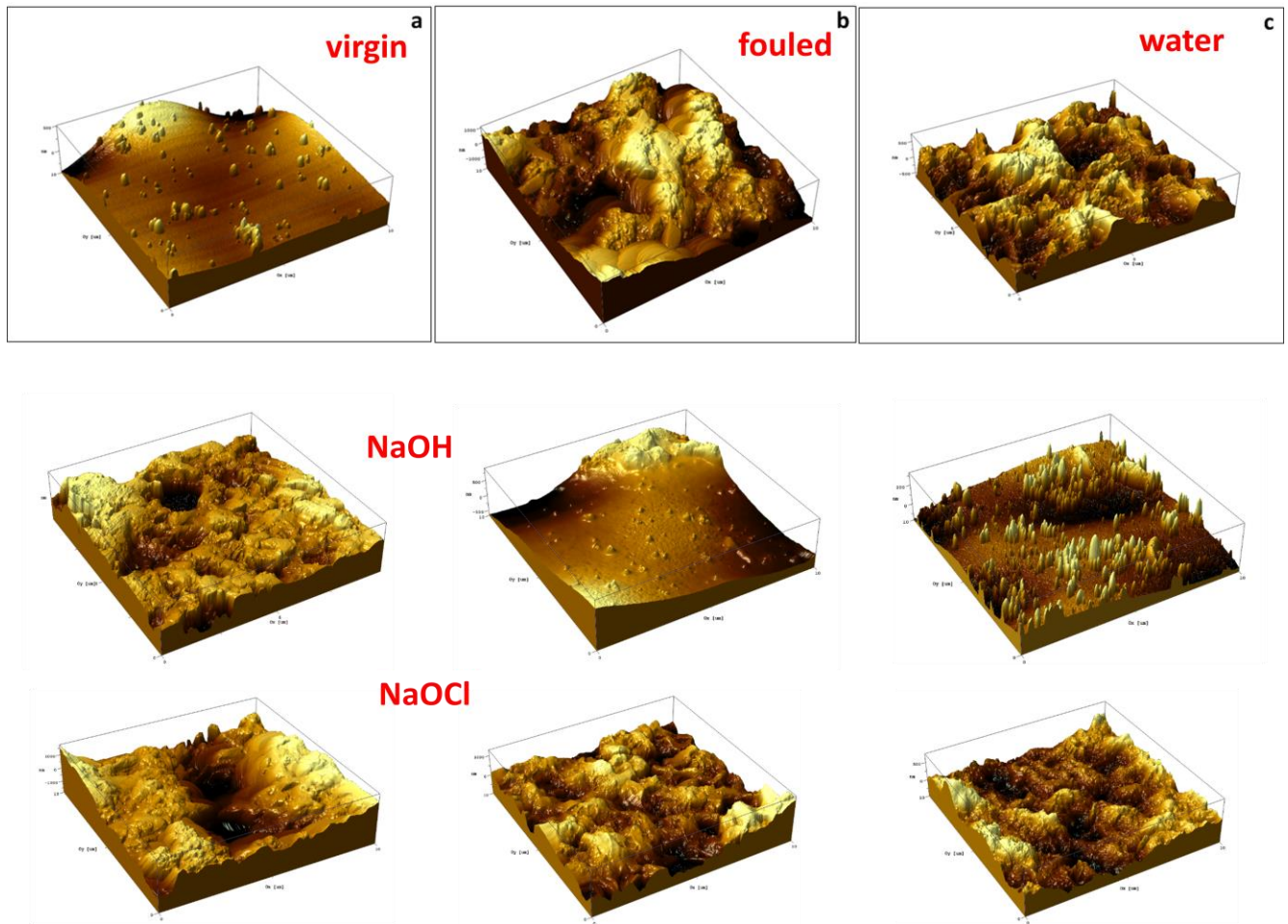
296

297   Figure 6. AFM of pristine (top left), fouled (top middle), and water-cleaned (top right) PES-300.

298   The middle row contains micrographs of the membrane cleaned with 1 (middle left), 5 (centre), and 10

299   (middle right) mg/L NaOH. The bottom row is the PES-300 cleaned with 1 (bottom left), 5 (bottom

300   middle), and 10 (bottom right) mg/L NaOCl.

301   As expected, the pristine membrane had the smoothest top layer [34,35]. The roughness of a fouled

302   membrane is 1 μm; this is 400 nm thicker than the roughness of the pristine membrane. The higher

303   roughness was evident through the larger differences between the bright and dark surface regions,

304   indicating the highest membrane surface points and membrane pores. Hydraulic cleaning with water

305   restored the roughness to 600 nm and left patches of fouling materials on the membrane surface. The

306   most effective cleaning agent in terms of membrane roughness was chemical cleaning with 10 mg/L

307   NaOCl. The roughness of the fouling layer was 500 nm; this is lower than the roughness of the pristine

308   membrane. Roughness gradually decreased from 1000 nm after cleaning with 1 mg/L NaOCl, to 800

309   nm with 5 mg/L NaOCl, to 500 nm with 10 mg/L NaOCl. After all three cleans, the membrane surface

310   remained replete with foulant residues. According to AFM, NaOCl cleaning agents concurrently attack

311   the foulants and the membrane. The results of the attack are a partial destruction of the organics and a

312   modified membrane surface. Complete destruction of proteins is achieved with NaOH, resulting in a

313   smooth surface with few remaining residuals.

314   Figure 7 illustrates the changes in the contact angle values of the pristine, fouled, and cleaned

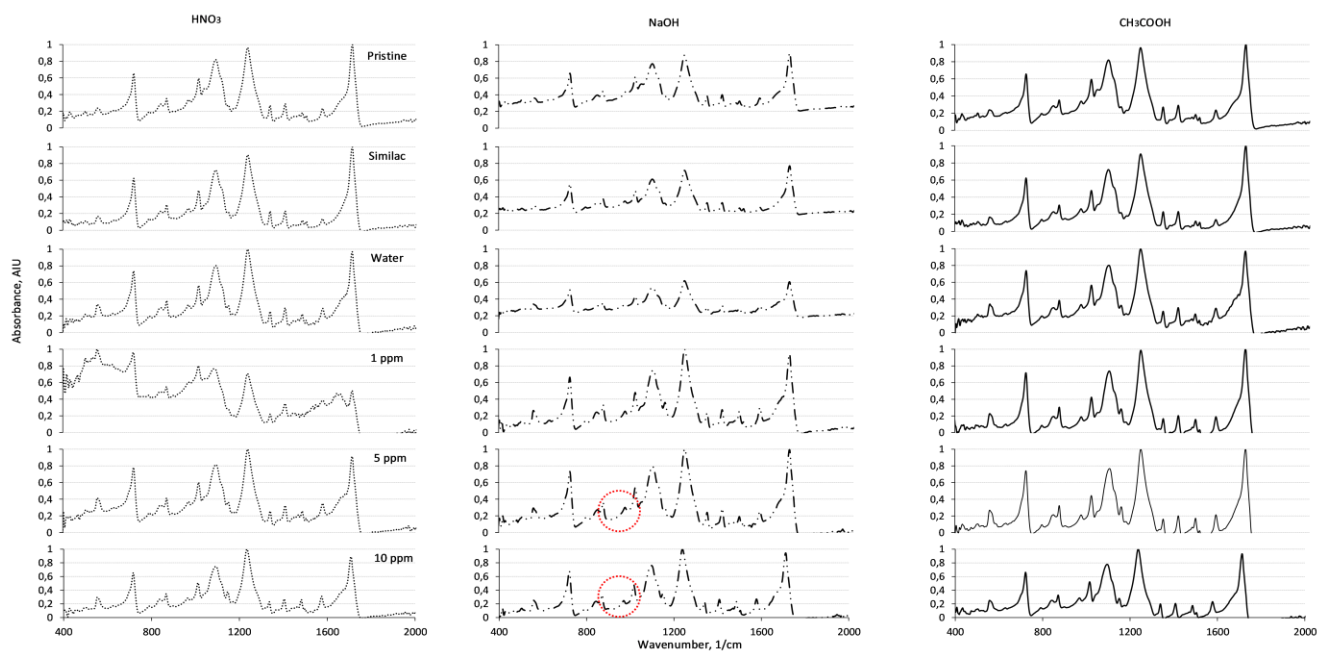315   membranes as a function of the cleaning agent concentration.
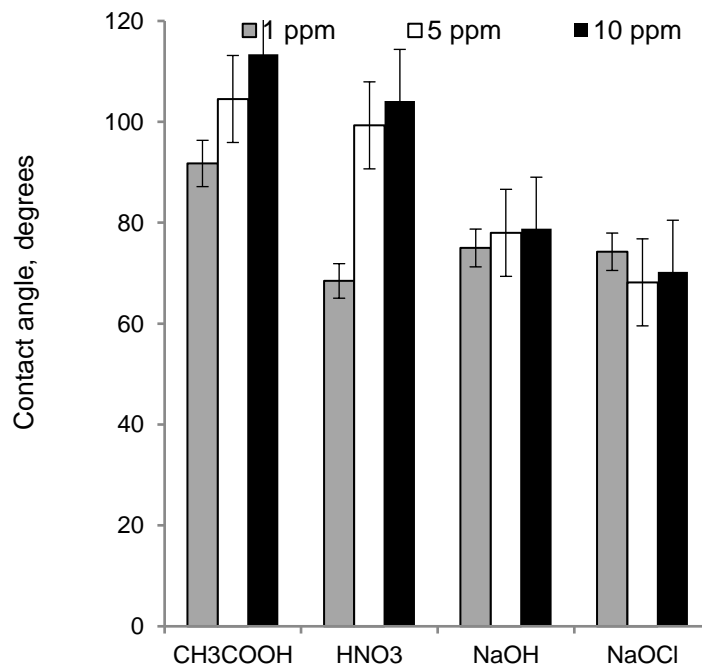
316

317   Figure 7. Contact angle of virgin, fouled, and cleaned membranes.

318   The lowest contact angle of 68°±3° was observed for the pristine membranes, while fouling

319   significantly increased the contact angle to 83°±4°. Hydraulic cleaning with water further increased the

320 contact angle to $100°±5°$. Cleaning with CH_3COOH and HNO_3 was unsuccessful; there were higher

321 contact angles of up to $113°±4°$ and $104°±3°$ for CH_3COOH and HNO_3, respectively, at the highest

322 cleaning doses. This suggests that acidic cleaning is not an appropriate approach for the removal of

323 organic foulants. For NaOH, cleaning with 1 mg/L resulted in a contact angle of $75°±3°$; this is slightly

324 higher than the contact angle of the pristine membrane. A $78°±3°$ contact angle was observed in the

325 membrane cleaned with 5 and 10 mg/L NaOH. NaOH efficiently lysed the foulant polymers [36] and

326 resulted in their complete removal from the membrane surface. Almost completely bare membrane

327 surfaces after NaOH cleaning were observed in the relevant AFM micrographs. A similar trend was

328 observed in the cleaning of fouled membranes with NaOCl. Cleaning with 1 mg/L NaOCl resulted in a

329 contact angle value of $74°±3°$, which is slightly higher than that of the pristine membrane; contact

330 angles of $68°±3°$ and $70°±3°$, respectively, were observed when the NaOCl concentrations were 5 and

331 10 mg/L. The difference between the contact angles for these membranes and the pristine membrane is

332 statistically insignificant and suggests that membranes were cleaned efficiently. Based on the observed

333 trends, the most successful cleans were conducted with NaOH and NaOCl. Relatively minor

334 differences in the observed contact angle values do not permit the formulation of specific

335 recommendations.

336 Previous studies on fouled membranes have not focussed on changes in the contact angle values. In

337 addition, contact angle measurements were routinely conducted and reported as a part of a

338 comprehensive characterisation of pristine and fouled membranes. Changes in contact angle values as

339 a function of fouling matter, the thickness, and charge [37] were counterbalanced by changes in

340 membrane roughness [38] measured with AFM. It is difficult to determine the exact reason that leads

341 to changes in the contact angle values; it is easy to correlate these changes with membrane roughness.

342 Thoroughly cleaned smooth surfaces display values that are similar to the values for the pristine

343 membrane; this represents the characteristics of the membrane material. Insufficiently cleaned

344 membrane surfaces are rough and display contact angle values significantly higher than those of the

345 pristine membrane.

346 The chemical cleanliness of the membrane surface was examined using ATR-FTIR. The results are

347 presented in Figures 8 and 9.

Figure 8. ATR-FTIR spectra of pristine, fouled, and cleaned PES-300 membrane. The spectra set after HNO_3 (left), NaOH (middle), and CH_3COOH (right) cleanings show the pristine (top), Similac-fouled (second top), fouled and water-cleaned (third top), fouled and cleaned with 1 mg/L (third bottom), 5 mg/L (second bottom, and 10 mg/L (bottom) cleaning agent PES-300 membrane.
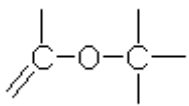
353
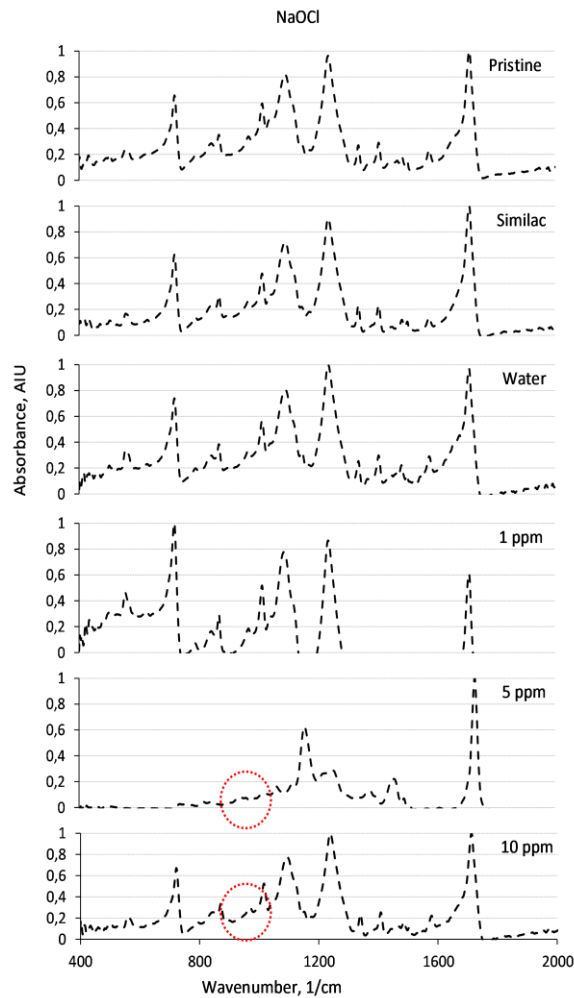
Figure 9. ATR-FTIR spectra of pristine, fouled, and NaOCl-cleaned PES-300 membrane. The set
shows ATR-FTIR spectra of pristine (top), Similac-fouled (second top), fouled and water-cleaned
(third top), fouled and cleaned with 1 mg/L (third bottom), 5 mg/L (second bottom, and 10 mg/L
(bottom) cleaning agent PES-300 membrane.

All samples showed a very broad band in the infrared (IR) range of 3300–3400 cm^{-1} (not shown in figure) typically associated with O-H vibrations in water and carbohydrate-like organic matter [39]. Other peaks associated with a pristine PES membrane reflected its structure consisting of a benzene ring, a sulfone group, and an ether bond [40]. Table 1 presents the IR absorption bands relevant to the PES structure.

363　　　　　　　　　Table 1. Assignment of relevant IR absorption bands to PES-300.

IR band, cm^{-1}	Range given in the literature [49], cm^{-1}	Assignment
555, 620, 915,	1000≤	Benzene rings

942, 990, 1000		
1030	About 1030	Benzene ring
1100	1085–1125	C-O stretching vibration
1150	1150 up to 1225	O-H deformation and C-O stretching vibration interaction
1250	1275–1200	$\diagup\!\!\!\!=\!\!C\!-\!O\!-\!C\!-$
1290	1300–1050	R-C-O-C-R
1320	1310–1350	SO_2
1485	1460–1550	C-S
1575	About 1580	Aromatic systems
1650	1580 up to 1660	C=C stretching vibration

Usually, peaks at 1240 cm^{-1} are ascribed to aromatic ethers and sulfonyl groups of PES. The peak at 1650 cm^{-1} corresponds to the C=C stretching vibration. The band at 717 cm^{-1} is due to the C-S groups; the bands at 1375 and 1109 cm^{-1} are attributable to the sulfone group, while the 1460–1470 cm^{-1} band is indicative of alkanes [41]. The IR spectral data of proteins consist of nine characteristic absorption bands of amides A, B, and I–VII. Table 2 presents the IR absorption bands of the proteins.

Table 2. Characteristics IR bands of proteins.

IR band, cm^{-1}	Designation	Description
200	Amide VII	Skeletal torsion
537–606	Amide VI	Out-of-plane C=O bending
625–767	Amide IV	OCN bending
640–800	Amide V	Out-of-plane NH bending
1229–1301	Amide III	CN stretching, NH bending
1480–1575	Amide II	CN stretching, NH bending
1600–1690	Amide I	C=O stretching
3100	Amide B	NH stretching
3300	Amide A	NH stretching

The protein fingerprints on the membrane surface may only be found if there is a lack of PES absorption bands in the desired IR range. Unfortunately, the amide II area of proteins (C-N and N-H bonds) overlapped with a strong peak at 1575 cm^{-1} assigned to the PES aromatic bond (Table 1). The amide I (carbonyl C=O bond) overlapped with the C=C stretching vibration band at 1650 cm^{-1}. The clearly observed trends are the disappearance of a band at 2270–2340 cm^{-1} (not shown in figure),

377   which corresponds to the N=C=O isocyanate group or C=N=O asymmetric stretch vibration. The band
378   was clearly observable in the virgin and Similac-fouled samples and disappeared after cleaning. The
379   band is attributed to polyvinylpyrrolidone (PVP), a preservative used to fill pores in the UF
380   membranes and create more hydrophilic membranes. The PVP was washed out during cleaning,
381   leaving a more hydrophobic membrane [42]. Another peak that had completely disappeared after
382   cleaning was located at 3400 cm^{-1} (not shown in figure), and was also attributed to organic
383   preservatives. Another band that appears in the virgin PES then disappears after fouling or cleaning
384   was located at 1070 cm^{-1}. This peak was attributed to O=S=O symmetric stretching [43,44]. Its gradual
385   disappearance indicates a possible chain scission of ether sulfone and the formation of phenyl
386   sulfonate. The mechanism of chain scission is usually explained by the deprotonation of -CH$_2$,
387   followed by the formation of C=C double bonds [14].

388   The contact angle, AFM, and ATR-FTIR provide important information regarding the efficiency of
389   chemical cleaning, although dismantling of a module is required for *off-situ* analysis. In the absence of
390   any solid reason, these methods will not be applied for a routine check of cleaning efficiency. This
391   leaves the evaluation of flux fluctuations. The surface properties of a membrane were not evaluated,
392   although they may be affected by cleaning. Zeta potential measurements provide additional useful
393   information on the surface state of the membrane. Figure 10 presents the zeta potential values of the
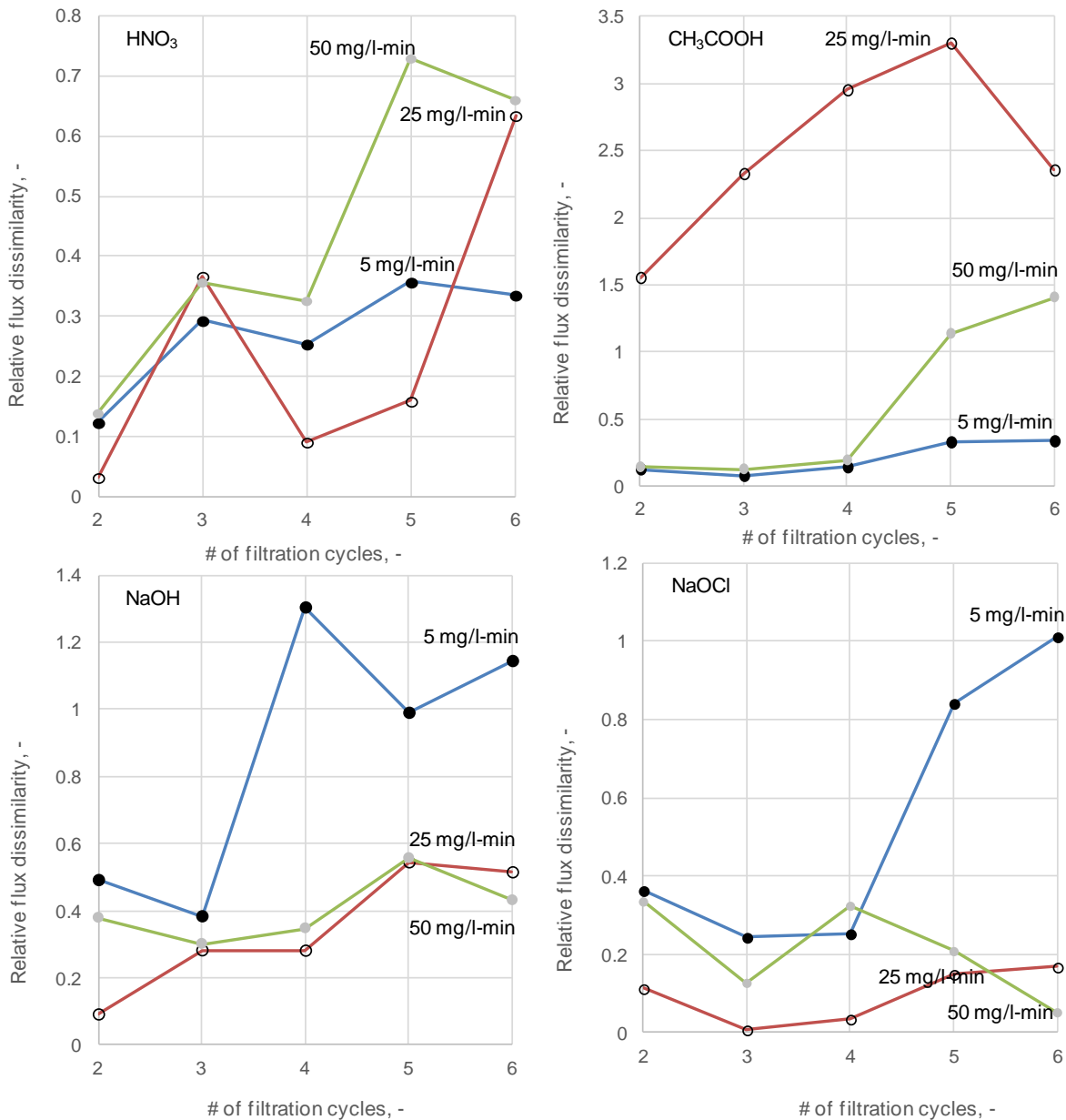394   pristine, fouled, and cleaned membranes.

395
396
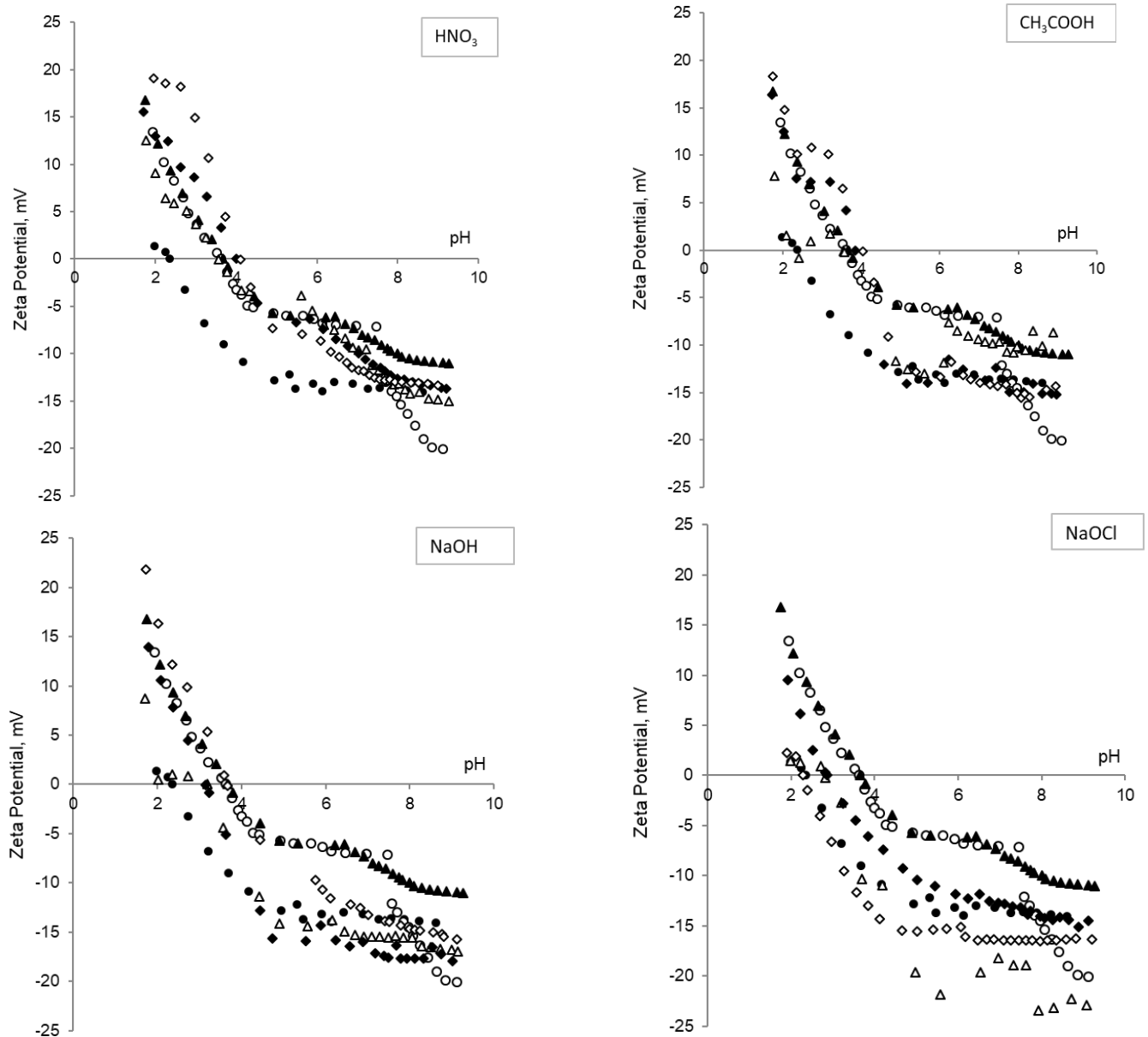
Figure 10. Zeta potential values of pristine (black circles), fouled (hollow circles), water-washed (black triangles), and cleaned with 1 (hollow triangles), 5 (black diamonds), and 10 (hollow diamonds) mg/L of HNO_3 (top left), CH_3COOH (top right), NaOH (bottom left), and NaOCl (bottom right) cleaning solution PES-300 membrane; the membrane was fouled with 0.6 g/L Similac 1 baby formula.

The zeta potential of the pristine membrane displayed slightly positive values at pH 2, had a point of zero charge (pzc) at pH 2.36, became increasingly negative until pH 6, and had a plateau at a pH higher than 6. The fouled membrane displayed a greater number of positive values, had a pzc at pH 3.6, maintained negative values of -5 mV until pH 7, and became increasingly negative until -20 mV at pH 9.1. The greater number of positive values were due to the adsorption of foulants on the membrane

406   surface [45]. Fouled membranes cleaned with water had zeta potential values similar to those of the
407   fouled membrane until pH 7, and slightly increased negative values towards -11 mV at pH 9.3.
408   Cleaning with 1 mg/L HNO_3 for 5 min resulted in a positive shift of zeta potential values, pzc at pH
409   3.57, and a slow decline of zeta potential values toward a plateau at -15 mV at pH ~9. Similar trends
410   with minor changes were observed in the zeta potential values for the membrane cleaned with 5 and 10
411   mg/L HNO_3. The trends closely resembled the values for cleaning with water with the exception of a
412   greater number of negative values at pH >6. The zeta potential values of PES-300 cleaned with
413   CH_3COOH were different from those observed for the pristine membrane although they were close to
414   each other and to the zeta potential values of HNO_3; the difference appeared in the positive values
415   largely found at higher acid doses. The cleaning resulted in 8, 16, and 18 mV at pH 1.7 for a fouled
416   membrane cleaned with 1, 5, and 10 mg/L CH_3COOH, respectively. These values rapidly decreased to
417   zero in the pzc of all three curves at pH 3.85, 4, and 4.1 for the same cleaning sequence. The zeta
418   potential of the membrane cleaned with 1 mg/L CH_3COOH became close to the values obtained after
419   cleaning the membrane with water. Cleaning with 5 and 10 mg/L CH_3COOH resulted in zeta potential
420   values similar to that of the pristine membrane at pH >6. Cleaning with NaOH resulted in more
421   positive zeta potential values at low pH, pzc at pH 3.2 for 1 and 5 mg/L NaOH, pzc at pH 3.6 for
422   cleaning with 10 mg/L NaOH, and more negative values for the cleaned membrane at pH >7. The zeta
423   potential values of the pristine membrane were around -12 mV, and those of the membranes cleaned
424   with NaOH at all three concentrations were approximately -17 mV for pH >6. A plateau in zeta
425   potential values was observed for the pristine as well as the NaOH-cleaned membranes, indicating the
426   adsorption equilibrium between the membrane surface and the bulk at a pH range [46]. The zeta
427   potential values observed after cleaning with NaOCl were very similar to the values of the pristine
428   membrane. The pzc of the pristine membrane was at pH 2.4. and the pzc for the cleaned membranes
429   was at pH 2.3–2.9. The values for the membrane cleaned with 1 mg/L NaOCl became more or less
430   trendy with the values of the pristine membrane. The values for the membrane cleaned with 10 mg/L
431   NaOCl were slightly more negative and displayed a plateau at -16 mV, and the values for the
432   membrane cleaned with 5 mg/L NaOCl were almost identical to those observed for the pristine
433   membrane.

434   Figure 11 depicts the cleaning efficiency assessed by the relative flux dissimilarity.

435

Figure 11. The efficiency of chemical cleaning assessed by the relative similarity in flux values of pristine, fouled, and cleaned membranes.

The fouling pattern at each run was compared to the fouling pattern during the first run conducted with the virgin membrane, and normalised by comparing the first run to a DIW run at 70 LMH. Efficient cleaning should result in the exact same fouling pattern for each consecutive run with low dissimilarity between runs. The relative dissimilarity in fluxes at the initial two runs was always approximately 0.3–0.4, meaning that the flow patterns differed by approximately 30–40%. After that, the dissimilarity shows various trends. Cleaning with HNO_3 resulted in a constant dissimilarity pattern at 5 mg/L·min, and increased dissimilarity was observed at 25 and 50 mg/L·min. According to the flux pattern,

445   although cleaning with HNO_3 may be conducted at 5 mg/L·min, this is not the case at 25 or 50

446   mg/L.min. The two latter concentrations produced a flux that was significantly different from the

447   initial fouling flux. An increasing relative dissimilarity suggests that the flux reduces toward negligible

448   values; as such, cleaning with high concentrations of HNO_3 is not advisable.

449   A similar conclusion was drawn when a fouled membrane was cleaned with CH_3COOH. A relative

450   dissimilarity value of up to 3.5 suggests that the only usable concentration of the cleaning agent was 5

451   mg/L CH_3COOH. The opposite was observed when cleaning with NaOH and NaOCl. Cleaning with

452   low concentrations of the cleaning agent produced a significantly different pattern with up to two-

453   times the dissimilarity between the initial fouling flux pattern and a pattern observed after six runs.

454   The relative dissimilarity in cleaning when using 25 and 50 mg/L NaOH was approximately 0.5, and

455   with NaOCl it was below 0.2. Based on these observations, better results are expected with 25 and 50

456   mg/L·min NaOCl. Other cleaning options that can be considered include 25 and 50 mg/L·min NaOH,

457   and 25 mg/L·min HNO_3 and CH_3COOH. These are typical observations which have been previously

458   reported. The cleaning of an UF membrane fouled by proteins with a liquid bleach is a classical

459   application. However, the observed trends can be further tuned by observing trends in the relative

460   dissimilarity of the zeta potential.

461   Figure 12 depicts the cleaning efficiency assessed by the relative dissimilarity of the zeta potential.
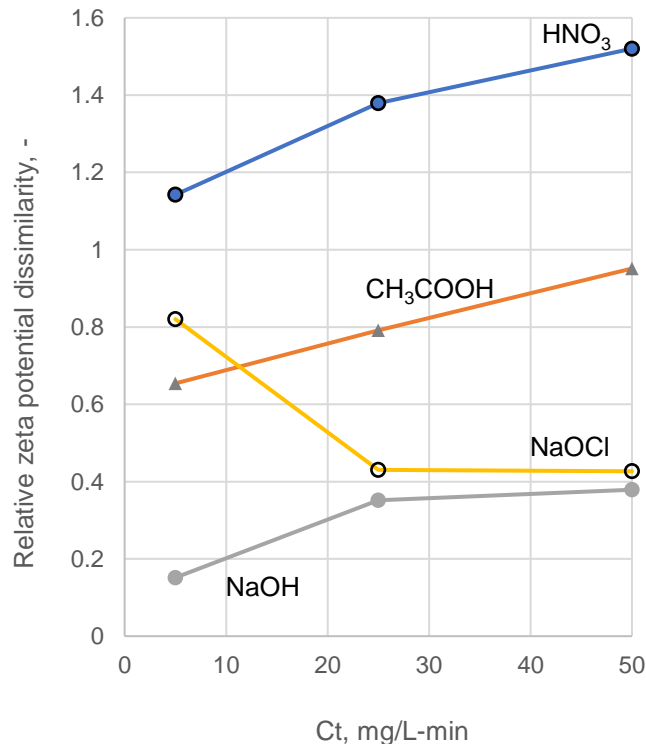
462

463   Figure 12. Cleaning efficiency as assessed by the dissimilarity in zeta potential values of the pristine
464   and cleaned membranes.

465   The dissimilarity in zeta potential values was calculated by comparing the zeta potential values of the
466   pristine and fouled-cleaned membranes at different pH levels. A higher difference in zeta potential
467   values indicates that the membrane remains fouled after cleaning. Cleaning with HNO_3 resulted in a
468   high dissimilarity between the pristine and cleaned membranes. Moreover, a higher concentration of a
469   cleaning agent increased this dissimilarity. A similar response was observed when the membrane was
470   cleaned with CH_3COOH, although this dissimilarity was observed at a smaller scale. Zeta potential
471   dissimilarities in the range of 0.6–1.5 indicate that the membrane has been completely fouled.
472   Cleaning with NaOH was the most successful when its concentration was 5 mg/L·min, although 25
473   and 50 mg/L·min NaOH also resulted in membrane cleaning. While cleaning with NaOCl could be
474   conducted with 25 and 50 mg/L·min NaOCl, this was not the case with 5 mg/L·min NaOCl; the zeta
475   potential difference was substantial. Combining the relative flux dissimilarity and zeta potential
476   difference narrows the appropriate range of cleaning procedures. First, it eliminates the option of
477   cleaning with 25 mg/L·min HNO_3 and CH_3COOH. Although the fouling pattern appears the same, the
478   zeta potential difference highlights the significant fouling that may be detected *in situ* and in the early
479   stages. The cleaning observed for 25 and 50 mg/L·min NaOH and NaOCl was similar. Cleaning may
480   be conducted with 25 mg/L·min of NaOH or NaOCl, making the cleaning safer and more
481   environmentally friendly.

482   **4. Discussion**

483   Chemical cleaning of the UF membranes is a part of daily membrane operation. Cleaning efficiency
484   was assessed using hydraulic tests that evaluate flux before and after the cleaning and through
485   numerous variations of the bubble point test. The latter is needed to ensure that cleaning did not affect
486   membrane integrity up to the extent at which the membrane contains pores larger than 1 μm. This is
487   critical for the effective disinfection by the UF membranes in terms of preventing the penetration of
488   bacteria typically larger than 1 μm. However, two other previously defined cleaning criteria, chemical
489   cleanliness (removal of all foulants, impurities, and residues of cleaning agents) and microbiological
490   cleanliness (absence of living microorganisms), are not typically evaluated [47]. However, chemical
491   cleaning is a complex interplay between foulants, cleaning agents, and membrane surfaces. This is
492   especially important for UF with polymer membranes that may be affected by the type and
493   concentration of the cleaning agent. Possible undesirable outcomes include insufficient cleaning that

494   maintains foulants on the membrane surface, sufficient cleaning that disintegrates the foulants while

495   preserving some organic matter on the membrane surface, and overcleaning that removes all foulants

496   and also modifies the membrane surface. These outcomes cannot be assessed by current tests that are

497   based on general knowledge and the monitoring of flux behaviour after cleaning; additional tests for

498   fine tuning of chemical cleaning are required, and these should be non-invasive, inexpensive, and

499   applicable *in situ.*

500   Membrane cleaning affects the permeability and zeta potential of polymer UF membranes. Zeta

501   potential values of protein-fouled membrane shift towards more positive values, suggesting that

502   organics are adsorbed on the membrane surface. The removal of organics by chemical cleaning

503   changes the zeta potential values back to those of a virgin membrane. A parallel evaluation of the zeta

504   potential with transmembrane flux can hint on one of three possible scenarios. When the zeta potential

505   values of a cleaned membrane are more positive than those of a virgin membrane, and flux is lower

506   than the flux through a pristine membrane, the membrane has been insufficiently cleaned although it is

507   still intact. When both zeta potential and flux values are similar to those of a pristine membrane, the

508   membrane is hydraulically and chemically clean, and remains intact. When the zeta potential values

509   are similar or more electronegative than the values of a pristine membrane, and the transmembrane

510   flux is higher than the flux through the pristine membrane, the membrane surface is altered. This

511   alteration may take a form of increased hydrophilicity, higher surface charge, or damage to the

512   membrane integrity. A pH-streaming potential profiling differentiates between regions where the

513   streaming potential curve of a fouled-cleaned membrane is above the curve of the pristine membrane,

514   close to it, or below it. Profiling also determines the preferable adsorption and cleaning zones. In our

515   study, the highest adsorption of foulants and the lowest efficiency of cleaning agents was observed

516   under acidic conditions. There was insufficient electrostatic repulsion between the two under neutral

517   conditions, and thus the possible removal of foulants from the membrane surface was due to chemical

518   disintegration. Effective removal under alkaline conditions was due to the combined effect of

519   denaturation and the electrostatic repulsion of mutually negatively charged membrane and foulants

520   [48].

521   Another especially valuable and relatively simple test is the modification of the Kolmogorov-

522   Smirnov test for data dissimilarities collected through flux or zeta potential measurements. The typical

523   approach is to compare the flux through a virgin membrane and a fouled-cleaned membrane. A higher

524   ratio of the latter to the former indicates a more cleaned membrane, while also signifying a more

525   modified membrane. The cleaning in this instance indicates a modification of the membrane surface in

526 terms of the removal of preservatives, or an increase in the membrane hydrophilicity through the

527 adjustment of membrane surface groups, or an enlargement of membrane pores. All these positive

528 effects are short and result in more severe fouling. Instead, exactly same fouling pattern and minimal

529 difference in streaming potential values of pristine and cleaned membranes indicate that the membrane

530 performs in the exact same manner time after time. And that is exactly what the test does. It is able to

531 compare the similarities in fouling patterns. The repetition of a pattern with minimal deviations

532 suggests that the cleaning procedure is optimal and may be maintained for a long period. Significant

533 deviations suggest that the cleaning procedure should be optimised. However, the flux measurements

534 are not sufficiently sensitive and need to be supported by another test; this is where the zeta potential

535 dissimilarity test comes into play. When the fouling dissimilarity pattern suggests multiple choices, the

536 zeta potential highlights the most prominent options. In this case, cleaning with 25 mg/L·min of NaOH

537 or NaOCl was found to be as efficient as cleaning with 50 mg/L·min NaOH or NaOCl. Applying half

538 doses of cleaning agents is a more economical and environmentally friendly procedure.

539 **5. Conclusions**

540 •   Parallel measurements of transmembrane flux and pH-streaming potential profiling of pristine and

541 chemically cleaned membranes are needed to develop site-specific cleaning protocols. The approach is

542 easy to implement, does not require expensive equipment, may be conducted *in situ*, and may be

543 expanded to address the efficiency of coagulation/flocculation. The expected benefits in implementing

544 the proposed approach include reduced cleaning time, reduced concentration of cleaning agents, and an

545 increased lifetime of the UF membranes.

546 •   A modified Kolmogorov-Smirnov test for dissimilarities in data collected through flux or

547 streaming potential measurements provides immediate, highly relevant statistical analysis to evaluate

548 the efficiency of the cleaning procedure.

549 •   Chemical cleaning of the fouled UF membranes may be tuned to address a specific composition of

550 the feed and become a site-specific procedure.

551

554 **6. References**

555 [1]   I. Levitsky, Y. Dahan, E. Arkhangelsky, V. Gitis, Retention of modified BSA by ultrafiltration
556   membranes, Journal of Chemical Technology and Biotechnology. 91 (2016) 400–407.
557   https://doi.org/10.1002/jctb.4588.

[2]   E. Arkhangelsky, I. Levitsky, V. Gitis, Retention of Biopolymers by Ultrafiltration Membranes, Chemical Engineering and Technology. 38 (2015) 2327–2334. https://doi.org/10.1002/ceat.201400775.

[3]   X. Shi, G. Tal, N.P. Hankins, V. Gitis, Fouling and cleaning of ultrafiltration membranes: A review, Journal of Water Process Engineering. 1 (2014) 121–138. https://doi.org/10.1016/j.jwpe.2014.04.003.

[4]   Z. Wang, J. Ma, C.Y. Tang, K. Kimura, Q. Wang, X. Han, Membrane cleaning in membrane bioreactors: A review, Journal of Membrane Science. 468 (2014) 276–307. https://doi.org/10.1016/j.memsci.2014.05.060.

[5]   I. Levitsky, A. Duek, E. Arkhangelsky, D. Pinchev, T. Kadoshian, H. Shetrit, R. Naim, V. Gitis, Understanding the oxidative cleaning of UF membranes, Journal of Membrane Science. 377 (2011) 206–213. https://doi.org/10.1016/j.memsci.2011.04.046.

[6]   V. Gitis, R.C. Haught, R.M. Clark, J. Gun, O. Lev, Application of nanoscale probes for the evaluation of the integrity of ultrafiltration membranes, Journal of Membrane Science. 276 (2006) 185–192. https://doi.org/10.1016/j.memsci.2005.09.055.

[7]   GE Healthcare, Cleaning of cross flow filtration membranes, Technical Brief 18-1171-72 AA, 2005.

[8]   Q. Gan, J.A. Howell, R.W. Field, R. England, M.R. Bird, M.T. McKechinie, Synergetic cleaning procedure for a ceramic membrane fouled by beer micro®ltration, Journal of Membrane Science. 155 (1999) 277–289.

[9]   M.A. Argüello, S. Álvarez, F.A. Riera, R. Álvarez, Utilization of enzymatic detergents to clean inorganic membranes fouled by whey proteins, Separation and Purification Technology. 41 (2005) 147–154. https://doi.org/10.1016/j.seppur.2004.05.005.

[10] P. Blanpain-Avet, J.F. Migdal, T. Bénézech, The effect of multiple fouling and cleaning cycles on a tubular ceramic microfiltration membrane fouled with a whey protein concentrate. Membrane performance and cleaning efficiency, Food and Bioproducts Processing. 82 (2004) 231–243. https://doi.org/10.1205/fbio.82.3.231.44182.

[11] G. Daufin, U. Merin, F.L. Kerherve, J.P. Labbe, A. Quemerais, C. Bousser, Efficiency of cleaning agents for an inorganic membrane after milk ultrafiltration, Key Engineering Materials. 61–62 (1991) 553–556. https://doi.org/10.4028/www.scientific.net/kem.61-62.553.

[12] R. Field, D. Hughes, Z. Cui, U. Tirlapur, Some observations on the chemical cleaning of fouled membranes, Desalination. 227 (2008) 132–138. https://doi.org/10.1016/j.desal.2007.08.004.

[13] C. Regula, E. Carretier, Y. Wyart, G. Gésan-Guiziou, A. Vincent, D. Boudot, P. Moulin, Chemical cleaning/disinfection and ageing of organic UF membranes: A review, Water Research. 56 (2014) 325–365. https://doi.org/10.1016/j.watres.2014.02.050.

[14] E. Arkhangelsky, D. Kuzmenko, V. Gitis, Impact of chemical cleaning on properties and functioning of polyethersulfone membranes, Journal of Membrane Science. 305 (2007) 176–184. https://doi.org/10.1016/j.memsci.2007.08.007.

[15] A. Weis, M.R. Bird, M. Nyström, The chemical cleaning of polymeric UF membranes fouled with spent sulphite liquor over multiple operational cycles, Journal of Membrane Science. 216 (2003) 67–79. https://doi.org/10.1016/S0376-7388(03)00047-4.

[16] A. Weis, M.R. Bird, M. Nyström, C. Wright, The influence of morphology, hydrophobicity and charge upon the long-term performance of ultrafiltration membranes fouled with spent sulphite liquor, Desalination. 175 (2005) 73–85. https://doi.org/10.1016/j.desal.2004.09.024.

[17] H. Zhu, M. Nyström, Cleaning results characterized by flux, streaming potential and FTIR measurements, Colloids and Surfaces A: Physicochemical and Engineering Aspects. 138 (1998) 309–321. https://doi.org/10.1016/S0927-7757(97)00072-1.

[18] D. Wu, M.R. Bird, The fouling and cleaning of ultrafiltration membranes during the filtration of model tea component solutions, Journal of Food Process Engineering. 30 (2007) 293–323. https://doi.org/10.1111/j.1745-4530.2007.00115.x.

[19] P.J. Evans, M.R. Bird, A. Pihlajamäki, M. Nyström, The influence of hydrophobicity, roughness and charge upon ultrafiltration membranes for black tea liquor clarification, Journal of Membrane Science. 313 (2008) 250–262. https://doi.org/10.1016/j.memsci.2008.01.010.

[20] M. Nyström, H. Zhu, Characterization of cleaning results using combined flux and streaming potential methods, Journal of Membrane Science. 131 (1997) 195–205. https://doi.org/10.1016/S0376-7388(97)00053-7.

[21] M. Pontié, X. Chasseray, D. Lemordant, J.M. Lainé, The streaming potential method for the characterization of ultrafiltration organic membranes and the control of cleaning treatments, Journal of Membrane Science. 129 (1997) 125–133. https://doi.org/10.1016/S0376-7388(96)00340-7.

[22] M. Pontié, L. Durand-Bourlier, D. Lemordant, J.M. Lainé, Control fouling and cleaning procedures of UF membranes by a streaming potential method, Separation and Purification Technology. 14 (1998) 1–11. https://doi.org/10.1016/S1383-5866(98)00054-9.

[23] J. Zeng, H. Ye, H. Liu, H. Xie, Characterization of a hollow-fiber ultrafiltration membrane and control of cleaning procedures by a streaming potential method, Desalination. 195 (2006) 226–234. https://doi.org/10.1016/j.desal.2005.12.003.

[24] A. Szymczyk, P. Fievet, J.C. Reggiani, J. Pagetti, Determination of the filtering layer electrokinetic properties of a multi-layer ceramic membrane, Desalination. 116 (1998) 81–88. https://doi.org/10.1016/S0011-9164(98)00059-9.

[25] N.D. Lawrence, J.M. Perera, M. Iyer, M.W. Hickey, G.W. Stevens, The use of streaming potential measurements to study the fouling and cleaning of ultrafiltration membranes, Separation and Purification Technology. 48 (2006) 106–112. https://doi.org/10.1016/j.seppur.2005.07.009.

[26] A. Al-Amoudi, P. Williams, S. Mandale, R.W. Lovitt, Cleaning results of new and fouled nanofiltration membrane characterized by zeta potential and permeability, Separation and Purification Technology. 54 (2007) 234–240. https://doi.org/10.1016/j.seppur.2006.09.014.

[27] H. Matsumoto, Y. Koyama, A. Tanioka, Interaction of proteins with weak amphoteric charged membrane surfaces: effect of pH, Journal of Colloid and Interface Science. 264 (2003) 82–88. https://doi.org/10.1016/S0021-9797(03)00417-X.

[28] M.Y. Jaffrin, L.H. Ding, Ch. Couvreur, P. Khari, Effect of ethanol on ultrafiltration of bovine albumin solutions with organic membranes, Journal of Membrane Science. 124 (1997) 233–241. https://doi.org/10.1016/S0376-7388(96)00241-4.

[29] N. Smirov, The Annals of Mathematical Statistics, The Annals of Mathematical Statistics. 19 (1948) 279–281. https://doi.org/10.1214/aoms/1177733256.

[30] R.W. Field, D. Wu, J.A. Howell, B.B. Gupta, Critical flux concept for microfiltration fouling, Journal of Membrane Science. 100 (1995) 259–272. https://doi.org/10.1016/0376-7388(94)00265-Z.

[31] P. Bacchin, P. Aimar, V. Sanchez, Model for colloidal fouling of membranes, AIChE Journal. 41 (1995) 368–376. https://doi.org/10.1002/aic.690410218.

[32] B. Espinasse, P. Bacchin, P. Aimar, Filtration method characterizing the reversibility of colloidal fouling layers at a membrane surface: Analysis through critical flux and osmotic pressure, Journal of Colloid and Interface Science. 320 (2008) 483–490. https://doi.org/10.1016/j.jcis.2008.01.023.

[33] B. Espinasse, P. Bacchin, P. Aimar, On an experimental method to measure critical flux in ultrafiltration, Desalination. 146 (2002) 91–96. https://doi.org/10.1016/S0011-9164(02)00495-2.

[34] D. Kuzmenko, E. Arkhangelsky, S. Belfer, V. Freger, V. Gitis, Chemical cleaning of UF membranes fouled by BSA, Desalination. 179 (2005) 323–333. https://doi.org/10.1016/j.desal.2004.11.078.

654 [35] I.N.H.M. Amin, A.W. Mohammad, M. Markom, L.C. Peng, N. Hilal, Flux decline study during
655   ultrafiltration of glycerin-rich fatty acid solutions, Journal of Membrane Science. 351 (2010) 75–
656   86. https://doi.org/10.1016/j.memsci.2010.01.033.

657 [36] R. Zhang, S. Yu, W. Shi, J. Tian, L. Jin, B. Zhang, L. Li, Z. Zhang, Optimization of a membrane
658   cleaning strategy for advanced treatment of polymer flooding produced water by nanofiltration,
659   RSC Adv. 6 (2016) 28844–28853. https://doi.org/10.1039/C6RA01832G.

660 [37] M.T. Tsehaye, S. Velizarov, B. Van der Bruggen, Stability of polyethersulfone membranes to
661   oxidative agents: A review, Polymer Degradation and Stability. 157 (2018) 15–33.
662   https://doi.org/10.1016/j.polymdegradstab.2018.09.004.

663 [38] M. Ji, X. Chen, J. Luo, Y. Wan, Improved blood compatibility of polysulfone membrane by
664   anticoagulant protein immobilization, Colloids and Surfaces B: Biointerfaces. 175 (2019) 586–
665   595. https://doi.org/10.1016/j.colsurfb.2018.12.026.

666 [39] E. Smidt, P. Lechner, M. Schwanninger, G. Haberhauer, M.H. Gerzabek, Characterization of
667   Waste Organic Matter by FT-IR Spectroscopy: Application in Waste Science, Appl Spectrosc. 56
668   (2002) 1170–1175. https://doi.org/10.1366/000370202760295412.

669 [40] S.G. Salinas-Rodriguez, G.L. Amy, J.C. Schippers, M.D. Kennedy, The Modified Fouling Index
670   Ultrafiltration constant flux for assessing particulate/colloidal fouling of RO systems,
671   Desalination. 365 (2015) 79–91. https://doi.org/10.1016/j.desal.2015.02.018.

672 [41] B. Malczewska, A. Żak, Structural Changes and Operational Deterioration of the Uf
673   Polyethersulfone (Pes) Membrane Due to Chemical Cleaning, Scientific Reports. 9 (2019) 1–14.
674   https://doi.org/10.1038/s41598-018-36697-2.

675 [42] J. Marchese, M. Ponce, N.A. Ochoa, P. Prádanos, L. Palacio, A. Hernández, Fouling behaviour of
676   polyethersulfone UF membranes made with different PVP, Journal of Membrane Science. 211
677   (2003) 1–11. https://doi.org/10.1016/S0376-7388(02)00260-0.

678 [43] S. Belfer, R. Fainchtain, Y. Purinson, O. Kedem, Surface characterization by FTIR-ATR
679   spectroscopy of polyethersulfone membranes-unmodified, modified and protein fouled, Journal
680   of Membrane Science. 172 (2000) 113–124. https://doi.org/10.1016/S0376-7388(00)00316-1.

681 [44] S. Sasikala, S. Meenakshi, S.D. Bhat, A.K. Sahu, Functionalized Bentonite clay-sPEEK based
682   composite membranes for direct methanol fuel cells, Electrochimica Acta. 135 (2014) 232–241.
683   https://doi.org/10.1016/j.electacta.2014.04.180.

684 [45] J. Liu, J. Xiong, X. Ju, B. Gao, L. Wang, M. Sillanpää, Streaming potential for identification of
685   foulants adsorption on PVDF membrane surface, Journal of Membrane Science. 566 (2018) 428–
686   434. https://doi.org/10.1016/j.memsci.2018.09.024.

687 [46] F. Luna-Vera, J.C. Alvarez, Adsorption kinetics of proteins in plastic microfluidic channels:
688   Real-time monitoring of lysozyme adsorption by pulsed streaming potentials, Biosensors and
689   Bioelectronics. 25 (2010) 1539–1543. https://doi.org/10.1016/j.bios.2009.11.002.

690 [47] P. Blanpain-Avet, J.F. Migdal, T. Bénézech, Chemical cleaning of a tubular ceramic
691   microfiltration membrane fouled with a whey protein concentrate suspension-Characterization of
692   hydraulic and chemical cleanliness, Journal of Membrane Science. 337 (2009) 153–174.
693   https://doi.org/10.1016/j.memsci.2009.03.033.

694 [48] M.M. Motsa, B.B. Mamba, A.R.D. Verliefde, Combined colloidal and organic fouling of FO
695   membranes: The influence of foulant–foulant interactions and ionic strength, Journal of
696   Membrane Science. 493 (2015) 539–548. https://doi.org/10.1016/j.memsci.2015.06.035.

697 [49] T. Maruyama, S. Katoh, M. Nakajima, H. Nabetani, T.P. Abbott, A. Shono, K. Satoh, FT-IR
698   analysis of BSA fouled on ultrafiltration and microfiltration membranes, Journal of Membrane
699   Science. 192 (2001) 201–207. https://doi.org/10.1016/S0376-7388(01)00502-6.

700